



A feasibility assessment of utilizing concentrated solar power (CSP) in the Zimbabwean regions of Hwange and Lupane

Bruce Mutume

Middle East Technical University, Sustainable Environment and Energy Systems Department, Kalkanlı, Guzelyurt, Mersin 10, Turkey

ARTICLE INFO

Keywords:

Zimbabwe
Concentrated solar power
Renewable energy
Analytic hierarchy process
Sustainability

ABSTRACT

The current study assesses the feasibility of Zimbabwe's Hwange and Lupane regions to host a large-scale Concentrated Solar Power (CSP) facility. The study's overarching goal is to aid in identifying, classifying, and validating suitable sites for hosting a CSP facility. In this paper, suitable sites are identified and classified by coupling the multi-criteria decision-making (MCDM) technique (specifically the analytical hierarchy process, abbreviated AHP) and geographic information system (GIS) software. Following the identification of suitable regions, the validation is carried out by technical and economic measures. As a specific criterion for decision-making, a geographic database was developed utilizing layers provided by various data sets on irradiance, orography, location, and water resources. The final maps using special tools in ArcGIS Pro revealed that the land available for concentrating solar power in Hwange and Lupane is 1792 km² (5.6% of the study area) and 3771 km² (11.9% of the study area), respectively. A Monte Carlo Simulation (MCS) of the theoretical power potential revealed that suitable sites in Hwange and Lupane could technically generate power ranging from 380.0 TWh/year to 477.5 TWh/year and 878.8 TWh/year to 1125.0 TWh/year, respectively. The CSP facility without a thermal energy storage (TES) facility has a \$ cost per kWh of 0.1879, while the CSP-TES hybrid costs 0.1468. The LCOE for CSP without TES and CSP with TES is \$ 0.0679 and \$ 0.0268 higher than Zimbabwe's electricity cost, respectively. Overall, results suggest that Lupane is an excellent location for CSP facilities and supports policymakers in establishing renewable energy tariffs, resulting in economic and sustainable development.

1. Introduction

The drastic climate change has bruised many countries with natural disasters such as droughts, floods, cyclones, etc. Irrespective of the fact that Zimbabwe emits a global share of 0.03% of fossil carbon dioxide (CO₂) (a principal constituent of global warming), the country has not been spared from the catastrophic events cultivated by global warming [1]. Therefore, every country must ensure that methods are strategized to reduce greenhouse gases (GHGs) for a sustainable environment.

With the 7th and 13th global sustainable development goals, the Zimbabwean government integrated climate change energy policies for Renewable Energy (RE) targets based on Nationally Determined Contributions (NDC). The RE targets were handed over to the United Nations Framework Convention on Climate Change (UNFCCC) [2]. The National Renewable Energy Policy of Zimbabwe (NREP) set targets for the RE types shown in Table 1. Renewable energy systems (RES) are considered the solution to a sustainable environment. Nonetheless, RES are still under development with significant drawbacks in efficiency, capacity factor, dispatchability,

E-mail address: bruce.mutume@metu.edu.tr.

<https://doi.org/10.1016/j.heliyon.2023.e18210>

Received 10 February 2023; Received in revised form 6 July 2023; Accepted 11 July 2023

Available online 13 July 2023

2405-8440/© 2023 Published by Elsevier Ltd.

This is an open access article under the CC BY-NC-ND license

(<http://creativecommons.org/licenses/by-nc-nd/4.0/>).

high capital cost, etc.

The 2250 MW target in Table 1 for large hydro is a flexible target that the Zimbabwean government could reduce to 1050 MW. Subsequently, the grid-solar capacity increases from 600 MW to 1800 MW [2]. The downsizing of hydro would make grid-solar the highest shareholder for RES in Zimbabwe, birthing opportunities for high-scale solar harvesting systems. Besides RES, the Zimbabwean government also proposed a new 600 MW coal-fuelled plant in the country's North-Western region [2].

The Zimbabwean power sector currently depends on four old and outdated coal-fuelled power plants, a hydro plant, and imported electricity. Of the 0.03% CO₂ share mentioned above, more than 70% of the GHG emissions in Zimbabwe are from the power industry [2]. Table 2 shows the power generation statistics for Zimbabwe as of March 2023. The inefficient coal-fuelled power plants generated approximately 7.3% of their total capacity. For decades, the Kariba power station has been the leading and sustainable source of electricity. However, owing to climate change, the water levels at Kariba have been decreasing with time. Toward the end of November 2022, Zimbabwe stopped generating electricity at the Kariba South Power Station of the Kariba Dam, birthing power outages lasting 19 h per day [3].

Currently, Zimbabwe faces the following energy-related challenges:

1. The release of GHGs from coal-fired power plants.
2. Energy poverty.
3. Power outages.

1.1. Previous work - Zimbabwe

Several studies on Zimbabwe's RE power sector have been conducted to increase the country's RE share or meet the grid-connected RE targets in Table 1. Below are some studies worth mentioning:

Chikwama et al. [5] assessed the geothermal energy potential of Lubimbi to host a 10 MW plant. Although the RE technology was established at a viable LCOE of 0.08 \$/kWh, Chikwama et al.'s [5] study did not consider the feasibility of generating electricity from a sizeable geothermal power plant, say over 100 MW. Considering generation statistics for Zimbabwe in Table 2, huge facilities must be considered in studies to solve power poverty effectively.

In a study to address electricity accessibility in Zimbabwe, Mhandu & Longe [6] assessed a solar-wind-diesel-storage hybrid system in some areas without electricity access. The authors established the hybrid system at an unfeasible electricity cost of 0.223 \$/kWh and a payback period of 5.6 years. Moreover, a study by Samu et al. [7] on the potential and feasibility of wind farms in Zimbabwe established that from 28 different locations in Zimbabwe, only 1 location had the most preferred results. In their study, Samu et al. [7] adopted the Gamesa G132-5.0 MW wind turbine, which has a low cut-in speed, suggesting how impractical it is to host wind farms in Zimbabwe. A wind-PV hybrid study by Samu et al. [8] concluded a resultant LCOE of 0.21 \$/kWh, which is hugely higher than Zimbabwe's retail cost of electricity (0.12 \$/kWh). So, including a PV system in a wind facility in Zimbabwe is not preferable because of the inadequate wind speeds.

Owing to the high solar irradiance in Zimbabwe, Chiteka & Enweremadu [9] assessed the development of solar photovoltaics (PV) in 30 locations of cities and towns. Chiteka & Enweremadu [9] developed a system that predicted optimal designs that reduced the cost of installation. Unfortunately, their study focused on off-grid solar installations, which are disadvantageous to an average Zimbabwean who cannot afford such systems (considering more than 50% of Zimbabweans earn below the poverty datum line). Nonetheless, a PV power potential study in Zimbabwe's 28 locations by Samu & Fahrioglu [10] revealed that all the locations were feasible. Nevertheless, a significant issue with their methodology is that the potential was established mainly on one criterion (i.e., irradiance), without including physical factors like land use, slope, proximity to road, grid, and other factors that can render the system unfeasible. Rashayi & Chikuni [11], in a study to analyze the potential of grid-connected PV in Zimbabwe, also considered irradiance as the only determining factor, among other technical factors, to validate the adoption via a LCOE value. In Zimbabwe's mining industry, Maronga et al.'s [12] evaluation of PV and CSP systems for power supply concluded that PV systems with battery storage offered the best performance, while CSP with TES offered tremendous potential for massive operations. A techno-economic analysis of a 32 MW CSP facility revealed the possibility for extensive CSP operations from Maronga et al. [12]. In 2014, Ziuku et al. [13] applied the GIS-MCDM methods to determine the potential of CSP in Zimbabwe and estimated power potential in most areas of the country. There are several potential factors for inaccuracy in their research. The primary discrepancy is that Zimbabwe's protected area coverage, as reported by UNEP-WCMC et al. [14], is 106 838 km². This coverage region represents all areas where CSP installations are not practical. Ziuku et al. [13] estimated that of Zimbabwe's total area of 390 760 km², the CSP eligible zones cover about 64%. Yet, 27% is not feasible (as

Table 1
Grid-connected RE targets [2].

Renewable energy type	Target (MW) by 2030
Large hydro	2250
Small hydro	153
Grid solar	600
Bagasse and other RE	275
Wind	100

Table 2
Zimbabwe generation statistics [4].

Location of facility	Power plant type	Capacity [MW]	Generated as of March 04, 2023 [MW]
Harare	Coal-fired	80	0
Bulawayo	Coal-fired	90	0
Munyati	Coal-fired	100	0
Hwange	Coal-fired	920	87
Kariba	Hydro-plant	1050	173

per UNEP-WCMC et al. [14]), without the inclusion of other factors that reduce the eligible zones like land used for residents and industries, sloppy regions, areas with insignificant irradiance, etc.

Various studies have been conducted to curb power poverty in Zimbabwe. All the studies reviewed so far, however, suffer from the fact that:

1. Considering Zimbabwe's unmet electricity demand, no study has analyzed a huge facility comparable and competitive to Zimbabwe's coal and hydropower stations. Considering Zimbabwe's RE targets mentioned in Table 1, studies focusing on meeting those targets are paramount.
2. Most studies established the potential of a RES by relying only on one physical factor (i.e., irradiance for PV and wind speed for wind farms), leaving other critical physical factors (e.g. available land area, topography, water resources, proximity to road structures and grid, soil structures, etc.).
3. For solar systems, most studies focused on PV systems, leaving the potential from large CSP operations undetermined.

1.2. Research objective

Accordingly, the current study investigates the potential of concentrating solar power from Zimbabwe's Hwange and Lupane regions. The Hwange and Lupane areas are chosen for study because they are famous for hosting most of Zimbabwe's coal reserves, coal bed methane (CBM), and high solar irradiance. Considering that, the region can be the potential for sustainable energy (through sustainable hybrid technologies) and development. The study investigates whether it is feasible to generate the 600 MW target from grid solar (Table 1) to help solve the country's energy-related challenges. Also, a 600 MW capacity is chosen to meet Zimbabwe's growing demand, as suggested by the Zimbabwean government's proposal of a 600 MW coal power plant. To meet the study's objectives, the following will be considered:

1. The multiple-criteria decision-making (MCDM) in geographic information system (GIS) software determines the most suitable locations from a chosen study area. Considering the studies mentioned in Section 1.1, the GIS-MCDM combination is a novel way to assess the viability of RES in Zimbabwe.
2. Studies reviewed in Section 1.1 focused on generating electricity from RES; however, they did not estimate the potential power from their areas of study. Therefore, the current study adopts a probabilistic Monte Carlo Simulation (MCS) approach to determine a range of potential power established at different (P90, P50, and P10) estimates. The probabilistic MCS approach, as compared to the deterministic approach, allows for more variation in the data, expressing the degree of uncertainty. This uncertainty is expressed by a range of values, where uncertainty reduces from the P10 (high) estimate to P50 (best), then the P90 (low) estimate.
3. The adoption of the System Advisor Model (SAM), a free techno-economic software model, for two cases: (1) a standalone CSP facility and (2) a CSP-Thermal Energy Storage (TES) hybrid.

In a nutshell, the study employs the GIS-MCDM combination coupled with the application of the MCS to determine the most appropriate sites for concentrating solar power from Zimbabwe's Hwange and Lupane areas. SAM is used to validate the techno-economic feasibility of concentrating solar power from the study area.

2. Concentrated solar power (CSP) technology

According to Roberts [15], solar PV contributes 2.4% against a combined 0.4% from geothermal, CSP, and ocean power of global electricity production's estimated renewable energy share. CSP and PV systems are similar in using the sun to generate power. However, as the aforementioned renewable energy shares suggest, PV systems are preferred. This section seeks to motivate the choice of the CSP system (against PV) and to provide a description of the CSP concept.

Since CSP systems can include a TES, storing energy as heat and using it to generate electricity during peak hours is feasible. On the other hand, for massive PV systems, it is challenging to store electrical energy. Electrical energy can be stored in electrochemical systems (such as batteries) or converted into other energy forms. Akbari et al. [16] summarized the storage technologies for PV as Electrical Energy Storage (EES) and TES, which depend on the energy's end-use.

Scholars have different opinions on which system (PV or CSP) is most feasible, considering storage facilities. PV systems are the most accepted and widely adopted technology, owing to being cheap and readily available for use, while CSP is less prevalent.

These are a few noteworthy viewpoints from the literature to motivate the adoption of CSP over PV systems:

Akbari et al. [16] outlined the electrical and thermal energy storage utilities for PV that could store energy ranging from 2 to 7.2 h and capacities ranging from 3.2 to 250 MWh. The authors concluded a preferred potential for PV with battery storage. Considering increased electrical demands lasting over the 7.2-h optima, some technologies Akbari et al. [16] presented do not support dispatchable electricity generation from RES.

In an outline of electrical energy storage for PV systems, Ibrahim et al. [17] highlighted the wide range of commercially available storage technologies under development and research. Therefore, it is still determining whether to gain reliance and assurance of the PV technology’s fundamental capabilities, capital, and operating costs.

Maronga et al. [12] evaluated PV and CSP systems to supply power for the mining sector in Zimbabwe and concluded that PV systems with battery storage offered preferred performance, while CSP with TES showed great potential for more extensive facilities.

Most literature on solar systems compares the growing and most preferred PV systems for small facilities (households, factories, farms, etc.) with the neglected CSP systems for huge facilities. However, Boretti & Castelletto [18] compared CSP and PV capacities greater than 100 MW. Boretti & Castelletto [18] considered dispatchability as an essential factor, and it justifies the adoption of CSP over PV systems. Boretti & Castelletto [18] compared the performance of a CSP parabolic trough (PT) plant without TES, and CSP PT with TES, with four PV power plants in America (all with capacities greater than 100 MW). Boretti & Castelletto [18] concluded that CSP without TES provided comparable performances at an acceptable cost, reaching the mass production of the current PV technologies.

Based on Maronga et al. [12] and Boretti & Castelletto [18], the current study focuses on determining the feasibility of concentrating solar power with/without TES in Zimbabwe’s Hwange and Lupane regions.

2.1. Concentrated solar power (CSP) concept

Parabolic troughs (PT), solar towers, and linear Fresnel generate electricity in CSP systems [19]. PT-based power plants are mature technologies that produce over 90% of the capacity belonging to CSP [20]. CSP PT technology uses mirrors called concentrators to focus thermal energy from the sun to the receivers called heat collectors or heat absorbers (see Fig. 1) [21]. The absorbers are long pipes located in the focus of the parabola. They accommodate the working fluid (WF), also known as a heat transfer fluid (HTF), which has a desired specific heat capacity, such as oil (whose capacity can reach 400 °C) or molten salt (550 °C). When the irradiance contacts the receivers, the WF absorbs the heat and becomes hot, reaching temperatures specific to the WF’s heat capacity [21]. The WF provides thermal energy to a heat exchanger to produce vapor, which then runs the steam turbine (ST), generating electricity. A condenser recycles the exhaust steam in the power generation systems. Fig. 1 shows the main components of the CSP PT system taken from EBSILON’s models.

The thermal ability of the CSP technology makes it possible to configure it to other thermal power plants to hybrid plants. Some CSP hybrids include CSP-PV, CSP-biomass, CSP-Wind, etc. The CSP system could also have a storage facility (e.g., the two-tank molten salt storage system in Fig. 1), CSP-TES hybrid.

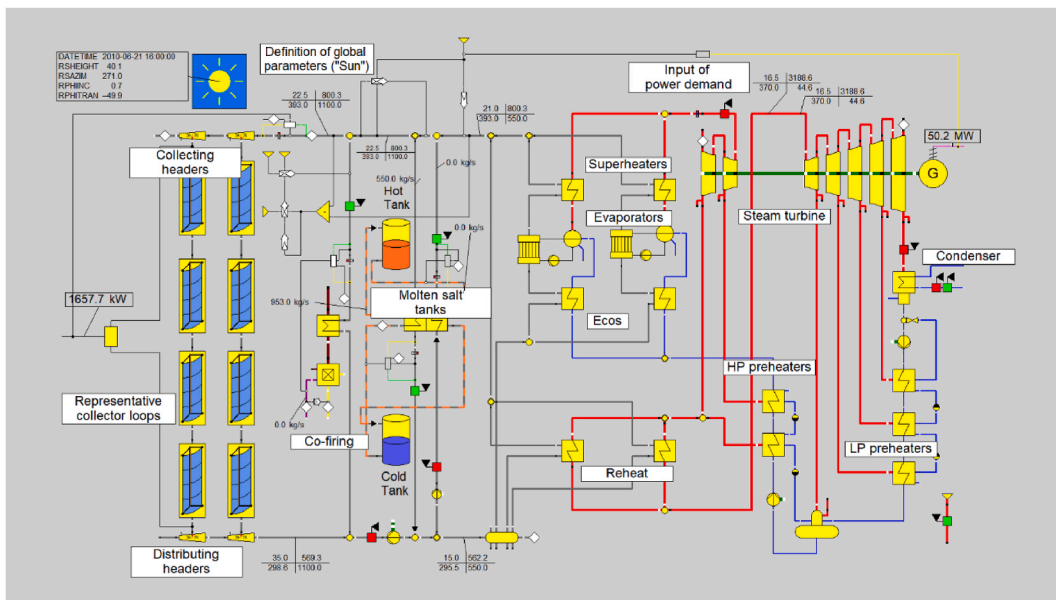


Fig. 1. EBSILON’s CSP PT schematic view [22].

2.2. Thermal energy storage (TES) technologies in CSP applications

According to Raul et al. [23], thermal energy can be stored for later utilization as sensible heat, latent heat, or thermo-chemical heat. However, sensible heat storage (SHS) materials are currently the most competent and extensively used in CSP plants [24]. The energy is stored in a TES material (liquid or solid) that changes temperature without changing phase or undergoing chemical reactions [24]. According to Equation (1), the heat capacity (mc_p) and temperature variation of the TES material (T) determine the amount of thermal energy stored (Q) as [24]:

$$Q = mc_p \times \Delta T \tag{1}$$

From Equation (1), the TES material should have a high specific heat capacity to store more thermal energy. So, choosing a TES material becomes an essential factor in CSP-TES systems. Among the many different TES materials, molten salts are the most mature and prevalently used in CSP plants for high-temperature SHS applications [24]. A thermocline-based system was proposed by Pacheco et al. [25] in contrast to the often-used two-tank molten salt storage system. The thermocline concept replaces more expensive molten salt with a less expensive filler material [25]. Regardless, according to the data published by the National Renewable Energy Laboratory (NREL) [26], the two-tank energy storage system is the most used for all CSP facilities globally. The storage system has a capacity ranging from 1 to 17.5 h [26], unlike the 2–7.2 h range for PV systems [16]. Table 3 shows some of the world’s operational PT CSP plants with two-tank storage systems.

3. Literature review on CSP site suitability

Concerning CSP systems, studies in Table 4 use GIS-MCDM methods to determine the suitability of concentrating solar power. The GIS-MCDM technique helps by displaying suitability with visual assistance. The Analytical Hierarchy Process (AHP) is the commonly applied method of the MCDM. Table 4 shows studies that applied the GIS-MCDM for CSP planning.

3.1. Multi-criteria decision-making (MCDM)/multiple-criteria decision analysis (MCDA)

Determining the most suitable location for CSP is a complex decision-making problem. The complexity is because there are many conflicting objectives and criteria to be considered. These conflicting criteria can include cost, quality measurement, and criteria selection. The MCDM/MCDA solves complex decisions for multiple-criteria decision-making challenges. While applying the MCDM, decision-makers can point out their preferences to differentiate between relative solutions or outcomes [30].

The AHP is the commonly applied planning method, as supported by the references in Table 4. The AHP organizes and analyzes options based on mathematics and psychology [35]. The technique helps decision-makers conclude their complex problems by comparing available options using selection criteria and sub-criteria [35].

Initially, the goal is defined, followed by criteria in the process. For example, the current study aims to find the most suitable site for concentrating solar power. The criteria are used to compare options from a variety of potential areas. The AHP applies a pairwise comparison to estimate weights for each criterion. Saaty [35] developed a table to show how one criterion could be more important than the other. Table 5 shows the AHP weighing scale, where each entry represents the importance of the i_{th} criterion to the j_{th} criterion. Furthermore, the relative importance of the j_{th} criterion to the i_{th} criterion is the reciprocal of a_{ij} , as shown in Table 5.

The following steps are taken when conducting the AHP,

1. Determine the goal of the analysis, and construct a decision hierarchy
2. Determine the criteria and sub-criteria
3. Assuming n criteria, set a pairwise comparison matrix $A [n \times n]$ [35]:

$$A = \begin{bmatrix} a_{11} & a_{12} & \dots & a_{1n} \\ a_{21} & a_{22} & \dots & a_{2n} \\ \dots & \dots & \dots & \dots \\ a_{n1} & a_{n2} & \dots & a_{nn} \end{bmatrix} \tag{2}$$

4. Get preference on the importance of each criterion against others based on the expertise of specialists and or literature.
 - a. Where, a_{ij} is the importance of the i_{th} criterion to the j_{th} criterion. The importance of the j_{th} term is $1/a_{ij}$.

Table 3
Operational PT CSP plants in the world with two-tank storage systems [26].

Station name	Country	Installed capacity (MWe)
Noor I Ouarzazate CSP Power Station	Morocco	160
Tonopah	USA	110
KaXu Solar One	South Africa	100
Andasol-1 (AS-1)	Spain	50
Delingha	China	50
Hassi R'mel Solar CC Power Plant	Algeria	20

Table 4
Studies using GIS-MCDM for CSP planning.

Study on	Country	Reference
CSP	Algeria	[27]
PV and CSP	China	[28]
CSP and PV	Iran	[29]
CSP	UAE	[30]
CSP	Morocco	[31]
CSP and PV	Morocco	[32]
CSP and PV	Tanzania	[33]
CSP and PV	Greece	[34]

Table 5
AHP importance scale [35].

Intensity Relative importance	Definition (<i>i</i> in respect of <i>i</i>)	Values a_{ij}	Numbers a_{ji}
1	Equal importance	1	1
2	Intermediate (between 1 and 3)	2	1/2
3	Moderate importance	3	1/3
4	Intermediate (between 3 and 5)	4	1/4
5	Strong importance	5	1/5
6	Intermediate (between 5 and 7)	6	1/6
7	Very strong importance	7	1/7
8	Intermediate (between 7 and 9)	8	1/8
9	Extreme importance	9	1/9

- b. The importance is based on the scale of importance by Saaty [35], shown in Table 5.
- 5. Matrix $A [n \times n]$ is normalized to matrix $[w_j]$ to obtain the weight for each criterion. The normalized priority vector is the division of the assigned numerical value by the sum of values in the same column. Finally, the average of each row is the weight for each criterion.
- 6. The consistency ratio (CR) checks or guarantees the consistency of judgments given by specialists or obtained from the literature. The CR must be less than 10% to satisfy consistency.
- a. The consistency ratio is given by [35]:

$$CR = \frac{CI}{RI} \tag{3}$$

- b. Where RI is the random index representing the deviation of matrices and is taken from Table 6. CI is the consistency index and is given by [35]:

$$CI = \frac{(\lambda_{max} - n)}{(n - 1)} \tag{4}$$

Table 6 shows Saaty’s [35] pairwise comparison indexes.

- c. Where λ_{max} is the maximum eigenvalue obtained from matrix $A (n \times n)$ and is given by [35]:

$$\lambda_{max} = \frac{\sum_j^n \left(\sum_{i=1}^n A_{ij} \right) w_j}{A_{ij}} \tag{5}$$

- 7. Finally, the land suitability index is computed as a result of integrating the AHP with GIS by [28]:

$$LSI_i = \sum_{j=1}^n w_j x_{ij} \times \prod_k^n EC_{ik} \tag{6}$$

Table 6
Random consistency indexes [35].

<i>n</i>	1	2	3	4	5	6	7	8	9	10	11	12
<i>RI</i>	0	0	0.58	0.9	1.12	1.24	1.32	1.41	1.45	1.49	1.51	1.54

- a. Where, LS_i is a land suitability index of area i , x_{ij} is the value of the area under the reclassification of j . w represents the assigned weight to the relative criterion j . EC_{ik} is the binary variable, such that if the respective area is under restricted areas, then $EC_{ik} = 0$, and installation for CSP is not feasible, otherwise $EC_{ik} = 1$.

4. Methodology and materials

4.1. Study area

The Hwange and Lupane regions (see Fig. 2) are an area of towns and cities in Matabeleland North province, the North-Western part of Zimbabwe. The Hwange and Lupane regions have an approximate area of 31 717 km², 8.1% of Zimbabwe's coverage area. Hwange, Kamativi, Dete, Kennedy, Lubimbi, Tshotsholo, Gwaai, and Lupane are all subsets of the research area. Due to high solar irradiance, vast coal resources, and the discovery of potential CBM, the study area has since provided some hope for secure and sustainable electricity generation. Mutume and Alp [36] estimated the CBM reserves in the North-Western region of Zimbabwe (see Fig. 2) and established that they ranged from 353 to 2850 billion cubic meters. Since methane is the cleanest fossil fuel, combining CBM and RES can offer Zimbabwe sustainable and competitive plant performance.

4.2. Framework methodology

Fig. 3 shows the methodology used in the current study to find the most appropriate location for concentrating solar power from Zimbabwe's Hwange and Lupane regions. Review and/or approval by an ethics committee was not needed for this study because the current study involves information freely available in the public domain, and the analysis of datasets, obtained from other researchers (where the data are properly anonymized).

GIS tools are combined with the multi-criteria decision-making method to determine the potential site for CSP systems. The methodology presented in Fig. 3 contains 8 main steps. Initially, the goal and criteria are defined in step (1), so unsuitable layers can be removed in step (2) accordingly with spatial tools in ArcGIS Pro (full-featured professional desktop GIS application). ArcGIS Pro software analyzes spatial data and performs exclusion and suitability analysis. At this point, we would have highlighted problematic areas, step (3) and, thus, potential rated sites, step (4). The AHP weights from step (5) are utilized in step (6) accordingly. In step (6), land suitability is performed in ArcGIS using GIS tools, resulting in a suitability map in step (7). The potential of CSP is analyzed and evaluated in step (8). Accordingly, a potential location for the CSP facility will be proposed to meet Zimbabwe's 600 MW NREP target (Table 1). A MCS is performed to estimate the power generation potential. Lastly, SAM is used to simulate the techno-economic potential of a 600 MW PT CSP facility.

4.2.1. Goal and criteria definition

The estimation for CSP potential requires more attention than the estimation for PV systems because, presently, CSP is one of the most expensive power-generating technologies. Thus, misjudgements can lead to tremendous economic penalties. Accordingly, the popularly defined criteria from the literature are adopted in the MCDM-AHP to identify the potential site and map out problematic areas.

4.2.2. The exclusion criteria of unsuitable locations or sites

Based on Fig. 3, the second step is to exclude all unsuitable sites for concentrating solar power based on logic and legal directives. According to Haddad et al. [27], Sun et al. [28], Ghasemi et al. [29], Alqaderi et al. [30], and Merrouni et al. [31], the excluded areas

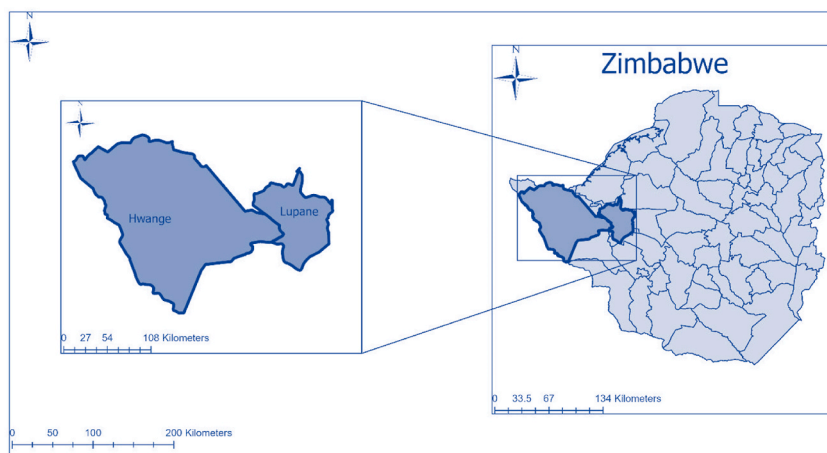


Fig. 2. The geographical location of Hwange and Lupane in Zimbabwe.

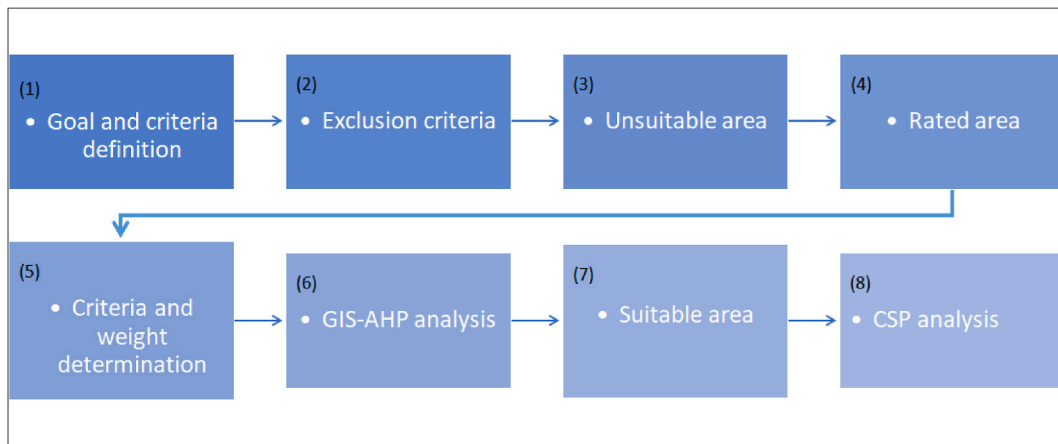


Fig. 3. Methodology for selecting suitable sites for concentrating solar power.

are summarized in Table 7. The criteria in Table 7 exclude all areas that might result in poor performance of the plant, destruction of essential sites, disturbance of the biosphere and ecosystem, high initial capital cost, increased maintenance cost, and the disruption of ongoing activities.

After excluding the layers in Table 7 and defining the rated area, Fig. 3 step (4), the fifth step evaluates the CSP plant site selection criteria based on a literature review (Table 4).

4.3. Criteria description

Based on the literature given by the sources in Table 4, climate, orography, location, and water availability assured maximum plant performance, territorial efficiency, and maximum achievable productivity. Table 8 shows the sources of the criteria used in the AHP.

4.3.1. Data collection

The current study performs relevant data searches (Table 8) and standardization (using ArcGIS Pro). The collected data is collected as spatial data and is normalized. Data is collected in a Tag Image File Format (tiff) and is converted to digital formats using ArcToolBox in ArcGIS Pro. First, a shapefile representing the study area is created. Data management tools, conversion tools, and spatial analyst tools, among other tools, are used to create Figures representing the climate, orography, location, and water resources. The final figure shows the criteria within the created shapefile. Table 8 shows the criteria and data sources for determining the suitability map for CSP installations in Zimbabwe’s Hwange and Lupane regions.

4.3.2. Climate

The performance of CSP plants is significantly affected by DNI to generate electricity. The current study considers excluding regions, Fig. 3 step 2, with DNI values less than 1800 kWh/m²/year for financial and technical accounts. Areas with the greatest DNI would be considered the most appropriate after using the GIS-AHP method. The higher the irradiance, the higher the theoretical potential. Table 9 shows the solar resource and site selection ranges of cumulative annual solar DNI, typically for CSP.

4.3.3. Orography

Orography is a study concentrated on the detailed and precise description of mountains and elevated terrains like hills. Adopting CSP power plants (especially the employment of PT collectors) requires flat lands [31]. An area’s inclination determines a site’s acceptability [28]. According to Tazi et al. [32], the suitable slope should be less than 2.1%, with excellent slopes ranging between 0.5% and 1%.

Table 7
Exclusion criteria and averaged values.

Excluded layers	Buffer		Remarks
Protected areas	Heritage sites	300 m–500 m	No installation within 300 m of the site
	National parks	300 m–500 m	No installation within 300 m of the site
	Biosphere	300 m–500 m	No installation within 300 m of the site
	Conservation areas	300 m–500 m	No installation within 300 m of the site
Climate	DNI	<1800 kWh/m ² /year	Exclude zones with DNI less than 1800 kWh/m ² /year
Orography	Slope	>2.1%	Exclude zones having slopes high than 2.1%
Proximity	Power lines	200 km	Exclude zones 200 km from the power grid
	Water supply	30 km	Exclude areas 30 km away from the site

Table 8
Data used for CSP site selection.

Criterion	Reference
Climate	SolarGIS [37]
Orography	USGS, United States Geological Survey [38]
Power grid	Worldbank [39]
Roads	MapCruzin [40]
Water availability	Africa Groundwater Atlas [41]

Table 9
Solar resource and site selection [42].

Not recommended	$DNI \leq 1600 \text{ kWh/m}^2/\text{year}$
Recommended	$1600 \text{ kWh/m}^2/\text{year} \leq DNI \leq 2000 \text{ kWh/m}^2/\text{year}$
Better performance	$DNI \geq 2000 \text{ kWh/m}^2/\text{year}$

4.3.4. Location

Any power plant should be near a road network and an electricity grid. The reason for this is that it may be less expensive to transport workers and have a plant-grid connection. A plant near a power grid, roads, railways, and load demand areas has low capital and operating costs.

4.3.5. Water resources

Considering the proposed system is a CSP plant, water plays a crucial role in the ST cycle. Water is a cooling agent for cleaning the concentrators, especially in windy areas. Qoaider & Liqreina [43] highlight high water consumption in CSP systems and that 90% of the water is used for wet cooling while 10% is for cleaning. Therefore there is a need for water bodies close to the CSP facility.

After defining the criteria and determining the criteria weights, Fig. 3 step 5, ArcGIS Pro is used to perform the GIS-AHP. Equation (6) is used in step (6) of Fig. 3, resulting in a suitability map in step (7).

4.4. Techno-economic potential

Solar generation is generally classified as the theoretical, technical, and economic potential [29]. The theoretical potential is the net annual solar radiation in a suitable region. The technical potential considers the theoretical potential and solar power technologies, while the economic potential estimates the cost of investment in comparison with conventional energy sources. The power generation potential can be calculated by [28]:

$$TPSE = DNI \times EF \times A \tag{7}$$

where,

- TPSE- Technical potential of CSP plant, [kWh/year],
- DNI- Direct solar irradiance value, [kWh/m²/year],

Table 10
Parameters for modeling and simulation [44].

Parameter	Value/Type
DNI	7.61 kWh/m ² /day
Design gross output	600 MWe
TES system	Two-tank
Cold tank capacity	25 MW
Hot tank capacity	25 MW
Hours of storage	12 h
Loop inlet WF temperature	293 °C
Loop outlet WF temperature	391 °C
WF type	Therminol VP-1
WF min. operating temperature	12 °C
WF max. operating temperature	400 °C
Water usage per wash	0.7 L/m ² , aperture
Collectors	SkyFuel sky trough (80 mm OD receiver)
Receivers	Schott PTR80
Storage WF fluid	Hitec solar salt
Capital cost	5627 \$/kW
Fixed O & M	66 \$/kWh
Analysis period	25 years
Inflation rate	2.5%/year

EF- Efficiency for the solar system, [%],

A- Area available, [m²].

The efficiency of PT solar technology ranges from 15% to 21% [28,29].

NREL's SAM is used to evaluate the techno-economic potential of CSP. The input DNI data for the study area is taken from NREL's National Solar Radiation Database (NSRD).

SAM uses Equation (8) to estimate the Levelized Cost of Electricity (LCOE) in \$/kWh [44]:

$$LCOE = \frac{(FCR \times CC + FOC)}{AEP} + VOC \tag{8}$$

where,

FCR- Fixed charge rate, and is given by [44],

$$FCR = CRF \times PFF \times CFF \tag{9}$$

CRF- Capital recovery factor.

PFF-Project financing factor.

CFF- Construction financing factor.

CC- Capital cost, [\$].

FOC- Fixed operating cost, [\$].

VOC- Variable operating cost, [\$/kWh].

AEP- Annual electricity production, [kWh].

Table 10 shows the parameters for modeling and simulation considered in the techno-economic analysis in SAM.

Accordingly, Equations (7) and (8) are used to perform the techno-economic analysis.

5. Results and discussion

5.1. Exclusion results

According to UNEP-WCMC et al. [14], Zimbabwe has 232 protected areas spread around the country. These protected areas include nature reserves, national parks, wilderness areas, national monuments, recreation parks, safari areas, sanctuaries, wildlife management areas, botanical reserves, state forests, and protected forests. The Hwange and Lupane regions host over 25% of Zimbabwe's protected areas. Fig. 4 shows the distribution of protected areas over the study area, covering more than half.

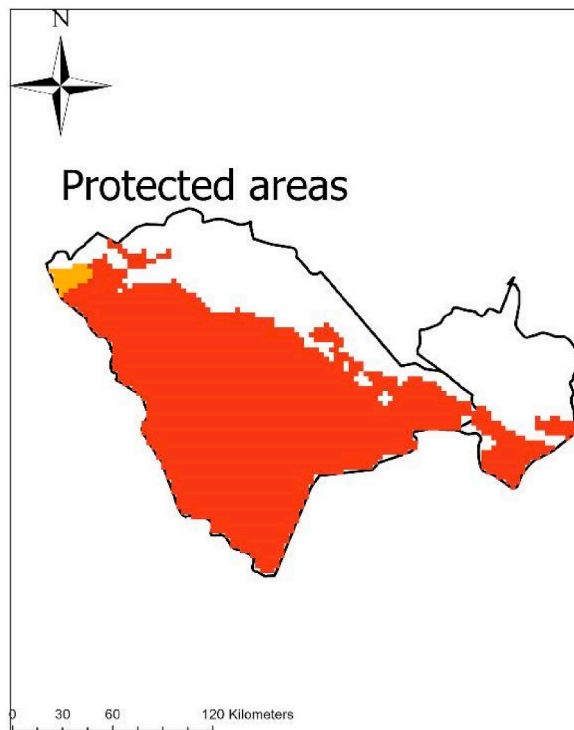


Fig. 4. Protected areas.

5.2. Criteria factors for the Hwange and Lupane areas

The data collected from references in Table 8 was standardized in ArcGIS Pro, and the following figures represent the physical factors of the Hwange and Lupane areas. Fig. 5 shows the DNI distribution over the study area, ranging from approximately 1800 to 2400 kWh/m²/year. Accordingly, there was no need to exclude regions with less than 1800 kWh/m²/year since the least DNI was exactly 1799.59 kWh/m²/year.

Figs. 6 and 7 are a representation of the standardized tiff digital elevation model data taken for the study area from USGS, United States Geological Survey [38]. Figs. 6 and 7 show the slope of the study area in meters and as a percentage, respectively. Most of the area has a slope of less than 2.1%, while the North areas of Hwange have slopes ranging between 5% and 10%.

Fig. 8 shows the land cover map of the Hwange and Lupane areas, where most of the land is covered with vegetation, which might be beneficial because most of the land would not be occupied or in use. Except in this case, the Hwange and Lupane regions host over a quarter of Zimbabwe’s protected areas.

Fig. 9 shows the road and electricity grid distribution, making the Southern part of Hwange less suitable for concentrating solar power as it is far from the grid and roads.

Fig. 10 shows the water resource distribution (mainly the Gwaii River) over the study area. The distribution also suggests less feasibility for the Southern part of Hwange as it is far from the water resources. Nonetheless, the Hwange and Lupane areas host most of Zimbabwe’s unconsolidated and sedimentary intergranular/fracture aquifer types. These aquifers have high groundwater potential, providing yields ranging between 10 m³/day/borehole and 5000 m³/day/borehole [41].

5.3. GIS-AHP results

The importance of each criterion is an average taken from consulting three specialists in RES and literature from Table 4. Table 11 shows the matrix [X], whereas Table 12 shows the normalized matrix [w] of matrix [X], with specified criteria weights.

The CR is calculated as shown below:

- $CR = \frac{CI}{RI}, CI = \frac{(\lambda_{max} - n)}{(n - 1)} = \frac{(4.190082 - 4)}{(4 - 1)} = 0.0633$
- $CR = \frac{CI}{RI} = \frac{0.0063361}{0.89} = 0.0712$

The CR is 7.1% (less than 10%), representing the collected data’s consistency. Accordingly, the weights in Table 12 are used in the GIS-AHP analysis. Solar irradiance (DNI) has the most weight at 55.5%, followed by the slope at 26.9%, proximity to the grid and road at 11.1%, and water resources at 6.6%.

Unsuitable regions were extracted, and Equation (6) was used to determine the land suitable for CSP operations. The latter was accomplished with the assistance of ArcGIS Pro analysis tools. The land available for concentrating solar power in Hwange and Lupane is 1792 km² and 3771 km², accounting for 5.6% and 11.9% of the Hwange and Lupane study area, respectively. The coordinates for the land available for CSP are shown in Table 13.

Most of the unsuitable area is in Hwange due to the constraints of the Hwange National Park and other protected areas, while most available land is in Lupane. Fig. 11 shows the land suitable for concentrating solar power in Hwange and Lupane. Accordingly, Lupane is chosen for CSP technologies.

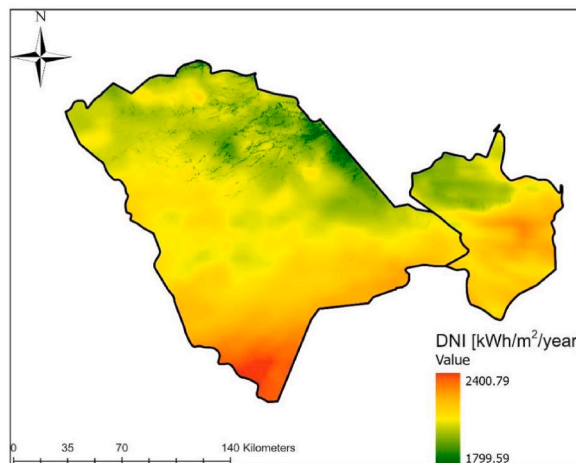


Fig. 5. Direct normal irradiance.

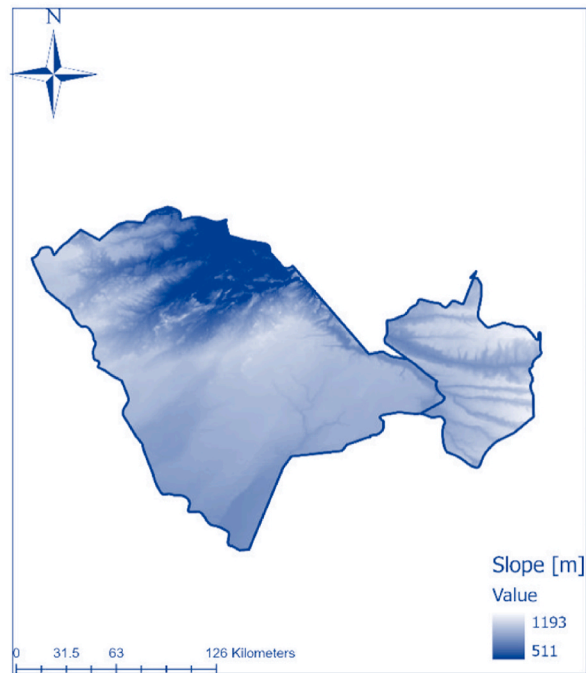


Fig. 6. Slope in meters.

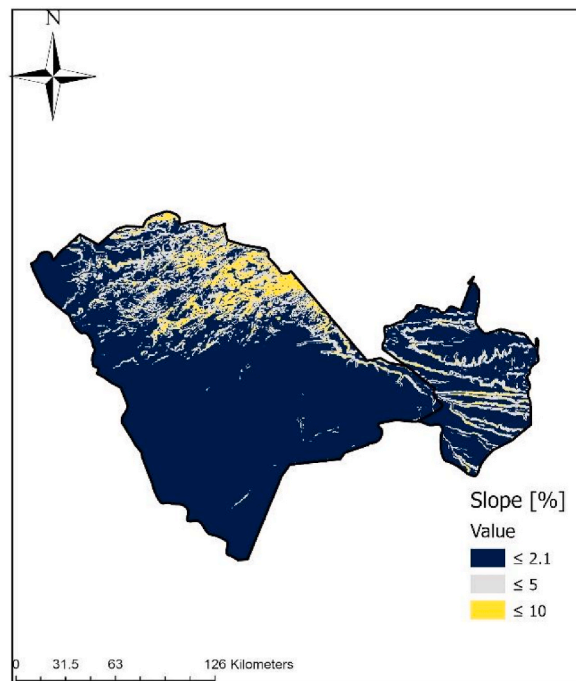


Fig. 7. Slope as a percentage.

5.4. Technical potential results

Equation (7) is used to calculate the technical power potential for both Hwange and Lupane. A MCS using Equation (7) is performed in MS Excel software [45]. A probabilistic approach using the MCS (with input variables DNI , EF , and A , according to Equation (7)) is used to estimate the range of values for the technical power potential ($TPSE$) because it reduces uncertainty in estimations. The DNI

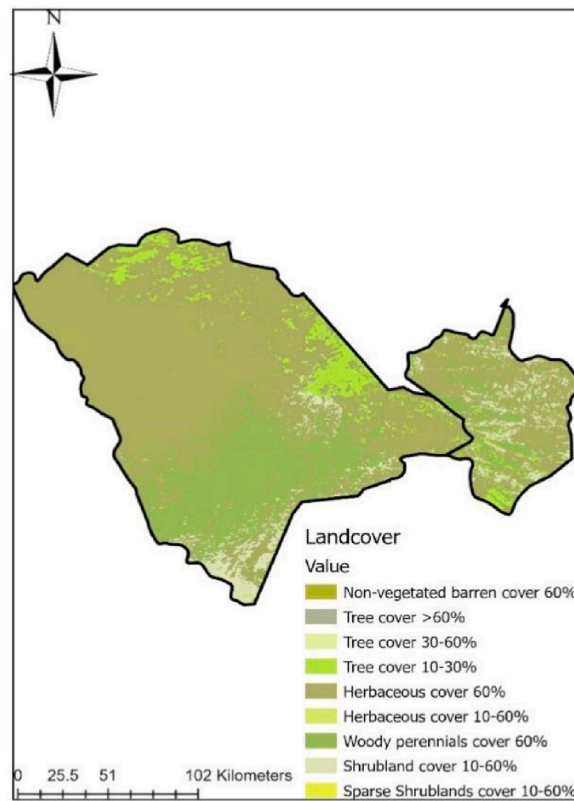


Fig. 8. Land cover.

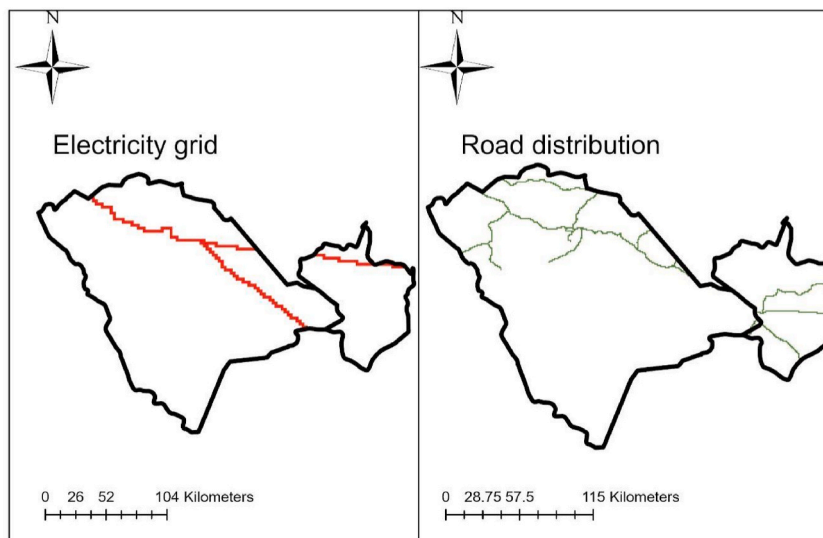


Fig. 9. Electricity grid and road distribution.

data range is from the specific suitable regions for CSP operations in Fig. 11. The efficiency range was estimated by modeling a 600 MW PT CSP plant with/without TES in SAM. Considering that SAM does not report an overall system efficiency, the overall incident irradiance to net power output was estimated by dividing the system power generated by the field thermal power incident after cosine. The area was taken from the suitability results in Section 5.3. Tables 14 and 15 show the summary statistics of the input (DNI , EF and A) used to estimate the output power potential ($TPSE$ for Hwange and Lupane, respectively).

Fig. 12(a) and (b) show the technical power distribution results for Lupane and Hwange, respectively. 100 000 combinations

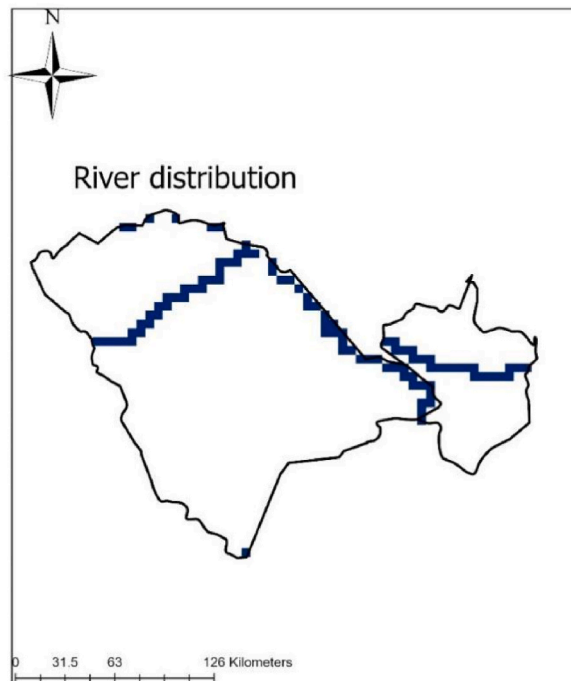


Fig. 10. Water resources.

Table 11
AHP matrix [X].

	Solar irradiance	Slope	Proximity	Water resources
Solar irradiance	1.0	3.3	5.2	5.9
Slope	0.3	1.0	4.0	4.3
Proximity	0.2	0.3	1.0	2.5
Water resources	0.2	0.2	0.4	1.0

Table 12
Normalized matrix [w].

	Solar irradiance	Slope	Proximity	Water resources	Weights [%]
Solar irradiance	0.6	0.7	0.5	0.4	55.5
Slope	0.2	0.2	0.4	0.3	26.9
Proximity	0.1	0.1	0.1	0.2	11.1
Water resources	0.1	0.1	0.0	0.1	6.6

Table 13
Coordinates of suitable land for concentrating solar power.

Area coordinate	City	
	Hwange	Lupane
1	26.3°E and 18.1°S	27.5°E and 18.6°S
2	26.9°E and 18.1°S	27.9°E and 18.4°S
3	26.3°E and 18.4°S	28.1°E and 19.3°S
4	26.9°E and 18.4°S	28.3°E and 18.8°S

produced more stable MCS results. The MCS for CSP power potential produced P10 (least likely generated), P50 (mid-case), and P90 (highest likely generated) values, as shown in Fig. 12. The theoretical power potential for the suitable area in Hwange and Lupane ranges from 380.0 TWh/year (P90) to 477.5 TWh/year (P10) and 878.8 TWh/year (P90) to 1125.0 TWh/year (P10), respectively, as shown in Table 16.

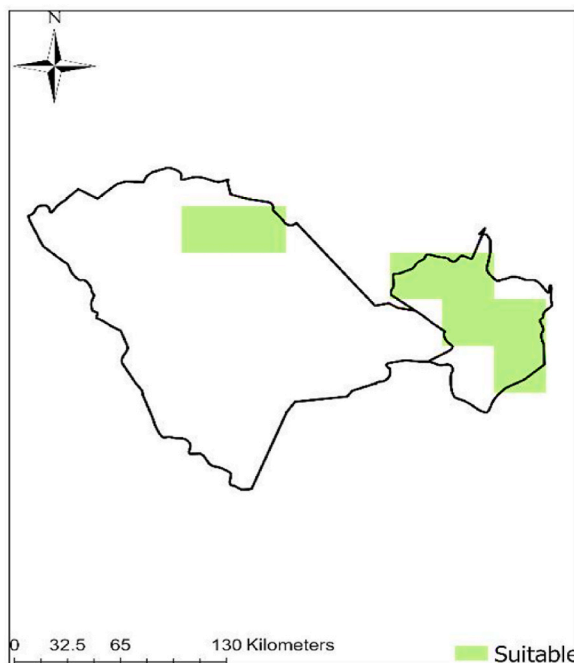


Fig. 11. Land suitability for concentrating solar power.

Table 14

Summary statistics used in MCS for the power potential of Hwange.

	Area [m ²]	DNI [kWh/m ² /year]	Efficiency [%]	TPSE [TWh/year]
Count	100 000	100 000	100 000	100 000
Average	1 792 000 000	1900.00	0.140	433.1
Minimum	1 792 000 000	1799.59	0.098	321.8
Maximum	1 792 000 000	2000.00	0.144	511.3
Type function	Constant	Triangular dis.	Triangular dis.	Cumulative dis. function

Table 15

Summary statistics used in MCS for the power potential of Lupane.

	Area [m ²]	DNI [kWh/m ² /year]	Efficiency [%]	TPSE [TWh/year]
Count	100 000	100 000	100 000	100 000
Average	3 771 000 000	2100.00	0.140	1007.5
Minimum	3 771 000 000	1900.00	0.098	715.7
Maximum	3 771 000 000	2300.00	0.144	1233.8
Type function	Constant	Triangular dis.	Triangular dis.	Cumulative dis. function

P90 indicates at least a 90% likelihood that the actual generated power will equal or surpass the low estimate. Accordingly, the estimated power potential in the current study for Hwange and Lupane is established at 380.0 TWh/year and 878.8 TWh/year, respectively. Lupane’s CSP potential is more than double that of Hwange. Considering that Lupane theoretically generates more electricity from CSP technologies, the techno-economic analysis for the district is carried out next.

5.5. Techno-economic results and discussion

The data in Table 10 is used in SAM to simulate the techno-economic potential of concentrating solar power in Lupane’s coordinated regions (Table 13). Considering the Zimbabwean government proposed NREP 600 MW grid solar target, the current study simulates a 600 MW PT CSP plant.

Fig. 13 shows the difference between CSP’s annual electrical power output with/without TES.

Accordingly, Fig. 13 shows the annual daily average electrical power output for CSP with/without TES. The results show that the power plant delivers a gross electrical power output at an annual average of 550 MW only between 10.00 a.m. and 4.00 p.m. The CSP plant without TES only generates significant amounts of electricity for an average of 7–8 h.

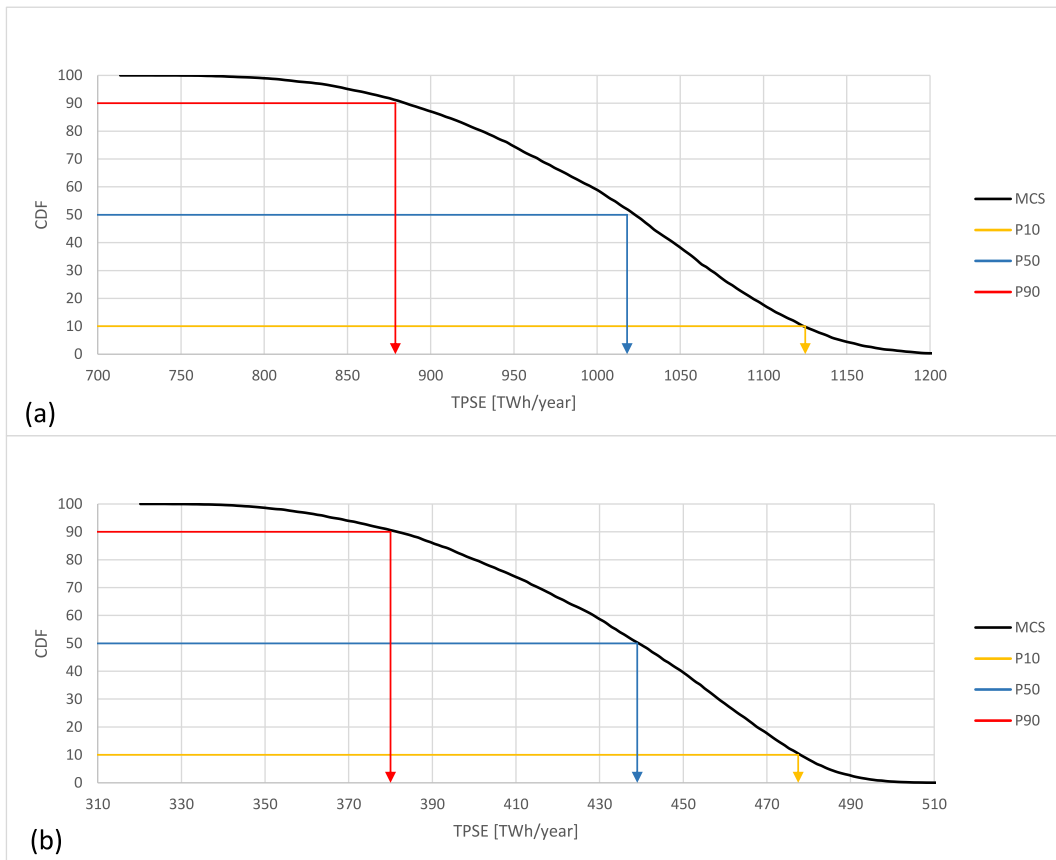


Fig. 12. The cumulative distribution function of TPSE values for Lupane (a) and Hwange (b).

Table 16
Range of TPSE in percentiles.

	TPSE [TWh/year] Percentiles		
	P10	P50	P90
Hwange	477.5	439.0	380.0
Lupane	1125.0	1018.0	878.8

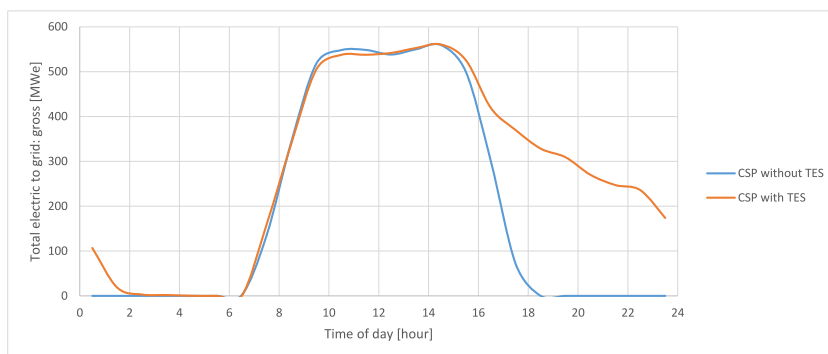


Fig. 13. Difference between the annual electrical power output for CSP with/without TES.

The 12-h two-tank TES facility increases the power output of the CSP power plant. However, the CSP-TES hybrid's electrical output dropped from 500 MW to 200 MW between 4.00 p.m. and 1:00 a.m. The decrease in electrical output is potentially caused by a variety of factors, including a decrease in direct normal irradiance, storage tank capacity, storage efficiency, exergetic efficiency, and heat losses, among others. The CSP-TES hybrid generates significant amounts of electricity for an average of 15–17 h. Thus, including a TES facility increases power generation, increasing the possibility of meeting the increased consumer demand.

Fig. 14 shows the energy output for the CSP plant with/without TES in kWh. The TES facility significantly increases the power output from March until October, while from November to February, there is insignificant change. In December, the CSP-TES hybrid generated less electricity than the CSP plant without TES. Numerous conditions must be met in TES facilities for optimal power block output. Given the decreased utilization for the TES due to the lowest heat output in December, the CSP-TES hybrid may have generated less energy output than the standalone CSP facility.

Table 17 compares the techno-economic results of a CSP facility with/without TES operating in Lupane of Zimbabwe.

LCOE for the CSP plant without TES and with TES is established at 0.1879 \$/kWh and 0.1468 \$/kWh, respectively. Results from Table 17 show that including a TES on a CSP facility reduces the cost of electricity by 22% while increasing the capacity factor by 29%. Results show that CSP technology consumes considerable amounts of water. So, water resources for the CSP technology can be accessed from Gwai River (see profile of water resources in Fig. 10), one of Zimbabwe's largest rivers. Also, considering that Lupane has aquifers yielding ranges between 10 m³/day/borehole and 5000 m³/day/borehole, it would require 1 to 10 wells to meet the annual water usage of the CSP plants in Table 17.

So, the facility has to be close to water resources: otherwise, the cost of electricity increases. According to Henbest et al. [46], Table 18 shows the LCOE ranges for the listed technologies in Zimbabwe.

Accordingly, results show that a CSP-TES hybrid in Lupane is preferable to onshore wind and solar PV while cost-competitive with biomass.

Zimbabwe's average generation and retail electricity costs are 0.11 \$/kWh and 0.12 \$/kWh, respectively [47,48]. The generation of electricity from CSP technologies is dismissed by economic consideration because both systems (with/without TES) generate electricity at a higher cost than the retail price of electricity in Zimbabwe. However, there is only a \$ 0.0268 difference between the retail price and the LCOE for the CSP-TES hybrid. The difference can be compensated by the financing conditions (incentives, interest rates, debt rates, etc.) associated with CSP technologies in Zimbabwe. The government of Zimbabwe can also guarantee viable power tariffs by introducing tariffs for renewable energy. Also, considering the incapacity of Zimbabwe's hydroelectric power plant in Kariba, the retail cost of electricity (0.12 \$/kWh) can increase, making the CSP-TES hybrid an economical technology for sustainable electricity generation. Moreover, Tables 17 and 18 show that a CSP-TES hybrid would be the most economical RES after small hydro.

Regardless of the higher than retail price LCOE value, a CSP plant avoids 820 gCO₂eq/kWh that would have been emitted by a 600 MW coal-fuelled power plant (see Introduction). The CSP's low capacity factor values (29.2–37.6%) compared to Zimbabwe's fossil fuel plants, whose capacity factor averages at 80%, account for the higher than retail price LCOE values. However, results show that the hybridization of a CSP plant with a storage facility significantly reduces the cost of electricity. The hybridization of CSP with fossil fuel power plants (such as combined cycle gas turbine plants and coal plants), in light of the fact that TES facilities are costly and only store energy rather than generate it, can thus significantly lower the cost of electricity to prices lower than Zimbabwe's retail prices.

6. Conclusions

This study aims to identify the most suitable location in the Hwang-Lupane area of Zimbabwe for concentrating solar power.

The combination of Geographic Information System maps and the Multiple-Criteria Decision Analysis- Analytic Hierarchy Process has been adopted to determine the most suitable areas for concentrating solar power. Through literature review, criteria for site selection are obtained, and a survey is carried out to get the weights for each criterion for the Analytic Hierarchy Process. Solar irradiance (DNI), slope, proximity to road and grid, and water resources are weighted at 55.5%, 26.9%, 11.1%, and 6.6%, respectively, using the AHP hierarchy structure and pairwise comparison. The coupling of the Geographic Information System and the Multiple-Criteria Decision Analysis is used to evaluate the most suitable site using spatial tools in ArcGIS Pro software. Maps for direct normal

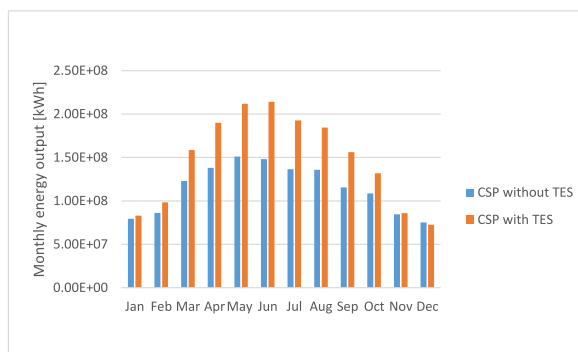


Fig. 14. Monthly energy output from Lupane's 600 MW CSP plant without TES.

Table 17
Techno-economic results of a CSP plant with/without TES in Lupane of Zimbabwe.

Metric	Value	
	CSP without TES	CSP-TES hybrid
Annual AC Energy in Year 1	1.4 TWh-e	1.8 TWh-e
Power cycle gross electrical output	1.7 TWh-e	2.5 TWh-e
Capacity factor	29.2%	37.6%
First-year kWh/kW	2559	3295
Annual water usage	398 019 m ³ /year	469 822 m ³ /year
Gross-to-net conversion	82.0%	72.2%
LCOE	0.1879 \$/kWh	0.1468 \$/kWh

Table 18
LCOE technology for Zimbabwe [46].

Technology	LCOE [\$/kWh]
Biomass	0.13–0.17
Small hydro	0.075–0.11
Solar PV	0.17–0.22
Onshore wind	0.18–0.22
Coal	0.079–0.096

irradiation, slope, land cover, water resources, road, and grid distribution are obtained to show regions with the most preferred physical parameters. The final suitability map indicates that the Lupane area has more suitable land for concentrating solar power. The land available for concentrating solar power in Hwange and Lupane is 1792 km² and 3771 km², respectively. This is so even when Hwange has more land coverage because Hwange hosts most of Zimbabwe's protected areas. As a result, Lupane is feasible for CSP technologies, while Hwange is less attractive (in comparison to Lupane). Nonetheless, Hwange has potential for CSP-fossil fuel hybrids, considering it hosts Zimbabwe's largest coal power plant.

A Monte Carlo Simulation is adopted to estimate the range of technical power potential for Hwange and Lupane. The theoretical power potential for the suitable area in Hwange and Lupane ranges from 380.0 TWh/year (P90) to 477.5 TWh/year (P10) and 878.8 TWh/year (P90) to 1125.0 TWh/year (P10), respectively

A techno-economic analysis for Lupane of a 600 MW CSP plant (with/without a thermal energy storage facility) is performed using NREL's System Advisor Model. The CSP-TES hybrid generates a gross electrical output of 0.28% of the theoretical power potential of Lupane's P90 estimate (878.8 TWh/year). The 0.28% indicates great potential for concentrating solar power in Lupane. However, the LCOE is higher than the retail cost of electricity in Zimbabwe, making generating electricity from a CSP plant less economically attractive. Since the cost of producing electricity from CSP plants is about twice as high as that from fossil-fuel plants, the LCOE calculations demonstrate that CSP facilities are not cost-competitive with conventional fossil-fuelled plants in Zimbabwe. The LCOE for the CSP plant without TES and with TES is established at 0.1879 \$/kWh, and 0.1468 \$/kWh, respectively. There is only a \$ 0.0268 difference between the retail price and the LCOE for the CSP-TES hybrid. The slight difference can be compensated by financing conditions (incentives, interest rates, debt rates, etc.) associated with CSP technologies in Zimbabwe.

Moreover, considering the inadequacy of Zimbabwe's hydroelectric power plant in Kariba, the retail price (0.12 \$/kWh) can increase, making CSP with TES a prudent technology of a feasible power era. Moreover, CSP technologies proved cost-competitive and preferable to other renewable energy systems in Zimbabwe. Results prove that generating electricity in Zimbabwe from a two-tank skyfuel sky trough CSP-TES hybrid is preferable over generating from biomass, wind, and solar PV.

In addition, the CSP-TES hybrid reduced the LCOE by 22%, suggesting better financial results for CSP-fossil fuel plant hybrids. The study shows the tremendous technical potential of CSP technologies in the Hwange and Lupane regions of Zimbabwe that can be utilized to check control power deficiencies and control GHG emissions. For financial potential, guaranteeing lower debt interest rates, among other economic variables, can lower the LCOE.

The current study's findings can potentially increase investments in solar energy systems in Zimbabwe's Hwange and Lupane regions, creating new jobs and ensuring the country's long-term development. Furthermore, the study's findings might increase the share of clean energy in the nation's energy mix. The results of this study can also guide domestic and international stakeholders in choosing optimal CSP locations that generate more electricity at a low cost. Further, the government can adopt the current study's findings to set up renewable energy tariffs, different from fossil fuel tariffs, to encourage renewable energy investment.

Further studies on the hybridization of renewable energy and typical fossil fuel plants are needed to analyze the change in the cost of electricity, GHGs, and power output.

Author contribution statement

Bruce Mutume: Conceived and designed the experiments; Performed the experiments; Analyzed and interpreted the data; Contributed reagents, materials, analysis tools or data; Wrote the paper. Data availability statement: No data was used for the research

described in the article.

Declaration of competing interest

The authors declare that they have no known competing financial interests or personal relationships that could have appeared to influence the work reported in this paper.

Acknowledgements

Author acknowledges use of library and IT resources of Middle East Technical University Northern Cyprus Campus during the time of MSc studies.

Nomenclature

Acronyms

AHP	Analytic hierarchy process
CBM	Coal bed methane
CSP	Concentrated solar power
EES	Electrical energy storage
GHG	Greenhouse gas
GIS	Geographic information systems
MCDA/MCDM	Multi-criteria decision analysis/making
MCS	Monte Carlo simulation
PT	Parabolic trough
PV	Photovoltaic
RE	Renewable energy
ST	Steam turbine
TES	Thermal energy storage
UNFCCC	United Nations Framework Convention on Climate Change
WF	Working fluid

Symbols

DNI	Direct normal irradiance, [kWh/m ² /year]
CR	Consistency ratio
CI	Consistency index
RI	Random index
λ_{max}	Maximum eigenvalue
n	Number of criteria
a_{ij}	Criteria matrix
w_j	Normalized from the matrix a_{ij}
LSI_i	Land suitability index
x_{ij}	The value of the area under the reclassification of j
EC_{ik}	Binary variable
$TPSE$	Technical potential of solar energy, [kWh/year]
EF	Efficiency of a solar system, [%]
A	Available area for solar energy, [m ²]

References

- [1] Zimbabwe CO2 Emissions - Worldometer'. <https://www.worldometers.info/co2-emissions/zimbabwe-co2-emissions/> (accessed December. 3, 2022).
- [2] National_Renewable_Energy_Policy_Final.pdf. Accessed: Dec. 02, 2022. [Online]. Available: https://www.zera.co.zw/National_Renewable_Energy_Policy_Final.pdf.
- [3] E. Chabuka, Intensive load shedding is imminent as Kariba lake levels are too low to generate electricity, Techzim (Nov. 27, 2022). <https://www.techzim.co.zw/2022/11/intensive-load-shedding-is-imminent-as-kariba-lake-levels-are-too-low-to-generate-electricity/>. (Accessed 8 December 2022).
- [4] Zimbabwe Power Company - Powering Zimbabwe into the future'. <https://www.zpc.co.zw/> (accessed December. 8, 2022).
- [5] N. Chikwama, M. M. Manyuchi, and N. Sukdeo, 'Techno-Economic Assessment for Geothermal Energy in Zimbabwe'.
- [6] S.R. Mhandu, O. Mary Longe, Techno-economic analysis of hybrid PV-Wind-Diesel-Battery standalone and grid-connected microgrid for rural electrification in Zimbabwe, in: 2022 IEEE Nigeria 4th International Conference on Disruptive Technologies for Sustainable Development (NIGERCON), Apr. 2022, pp. 1–5, <https://doi.org/10.1109/NIGERCON54645.2022.9803058>.
- [7] R. Samu, M. Fahrioglu, C. Ozansoy, The potential and economic viability of wind farms in Zimbabwe, Int. J. Green Energy 16 (15) (Dec. 2019) 1539–1546, <https://doi.org/10.1080/15435075.2019.1671424>.

- [8] R. Samu, M. Fahrioglu, O. Taylan, Feasibility study of a grid connected hybrid PV-wind power plant in Gwanda, Zimbabwe, in: 2016 HONET-ICT, Oct. 2016, pp. 122–126, <https://doi.org/10.1109/HONET.2016.7753434>.
- [9] K. Chiteka, C.C. Enweremadu, Development of a solar photovoltaic system sizing application for Zimbabwe, in: 2016 International Conference on Electrical, Electronics, and Optimization Techniques (ICEEOT), Mar. 2016, pp. 1018–1023, <https://doi.org/10.1109/ICEEOT.2016.7754840>.
- [10] R. Samu, M. Fahrioglu, An analysis on the potential of solar photovoltaic power, *Energy Sources B Energy Econ. Plann.* 12 (10) (Oct. 2017) 883–889, <https://doi.org/10.1080/15567249.2017.1319437>.
- [11] E. Rashayi, E. Chikuni, The potential of grid connected photovoltaic arrays in Zimbabwe, in: 2012 16th IEEE Mediterranean Electrotechnical Conference, Mar. 2012, pp. 285–288, <https://doi.org/10.1109/MELCON.2012.6196434>.
- [12] A. Maronga, K.J. Nyoni, P.G. Tuohy, A. Shane, Evaluation of PV and CSP systems to supply power in the Zimbabwe mining sector, *Energies* 14 (13) (Jan. 2021), 13, <https://doi.org/10.3390/en14133740>.
- [13] S. Ziuku, L. Seyitini, B. Mapurisa, D. Chikodzi, K. van Kuijk, Potential of concentrated solar power (CSP) in Zimbabwe, *Energy Sustain. Dev.* 23 (Dec. 2014) 220–227, <https://doi.org/10.1016/j.esd.2014.07.006>.
- [14] UNESCO-MAB, UNEP-WCMC, Zimbabwe Parks and Wildlife Management Authority, and Ramsar Secretariat, 'Protected Planet | Zimbabwe', *Protected Planet*, 2020. <https://www.protectedplanet.net/country/ZWE>. (Accessed 4 December 2022).
- [15] D. Roberts, The Global Transition to Clean Energy, Explained in 12 Charts, *Vox*, Jun. 18, 2019. <https://www.vox.com/energy-and-environment/2019/6/18/18681591/renewable-energy-china-solar-pv-jobs>. (Accessed 4 March 2023).
- [16] H. Akbari, et al., Efficient energy storage technologies for photovoltaic systems, *Sol. Energy* 192 (Nov. 2019) 144–168, <https://doi.org/10.1016/j.solener.2018.03.052>.
- [17] H. Ibrahim, R. Beguenane, A. Merabet, Technical and financial benefits of electrical energy storage, in: 2012 IEEE Electrical Power and Energy Conference, Oct. 2012, pp. 86–91, <https://doi.org/10.1109/EPEC.2012.6474985>.
- [18] A. Boretti, S. Castelletto, Cost and performance of CSP and PV plants of capacity above 100 MW operating in the United States of America, *Renew. Energy Focus* 39 (Dec. 2021) 90–98, <https://doi.org/10.1016/j.ref.2021.07.006>.
- [19] ferdi-p187-concentrated-solar-power-csp-and-photovoltaic-pv-has-time.pdf. Accessed: Dec. 02, 2022. [Online]. Available: <https://ferdi.fr/dl/df-adXANyWncqpaod8YwWbZWGtu/ferdi-p187-concentrated-solar-power-csp-and-photovoltaic-pv-has-time.pdf>.
- [20] Rao and Reddy - 2020 - Enhancement Of Energy Efficiency With Modeled Desi.pdf. Accessed: Dec. 02, 2022. [Online]. Available: <http://www.ijstr.org/final-print/apr2020/Enhancement-Of-Energy-Efficiency-With-Modeled-Design-Of-Concentrated-Solar-Power-Technology-Using-Parabolic-Dish-And-Trough.pdf>.
- [21] A. Berrada, K. Loudiyi, R. El Mrabet, Chapter 1 - introduction to hybrid energy systems, in: A. Berrada, R. El Mrabet (Eds.), *Hybrid Energy System Models*, Academic Press, 2021, pp. 1–43, <https://doi.org/10.1016/B978-0-12-821403-9.00001-9>.
- [22] 'Downloads', STEAG Epsilon. <https://www.epsilon.com/en/downloads> (accessed December. 9, 2022).
- [23] A. Raul, M. Jain, S. Gaikwad, S.K. Saha, Modelling and experimental study of latent heat thermal energy storage with encapsulated PCMs for solar thermal applications, *Appl. Therm. Eng.* 143 (Oct. 2018) 415–428, <https://doi.org/10.1016/j.applthermaleng.2018.07.123>.
- [24] O. Achkari, A. El Fadar, Latest developments on TES and CSP technologies – energy and environmental issues, applications and research trends, *Appl. Therm. Eng.* 167 (Feb. 2020), 114806, <https://doi.org/10.1016/j.applthermaleng.2019.114806>.
- [25] J.E. Pacheco, S.K. Showalter, W.J. Kolb, Development of a molten-salt thermocline storage system for parabolic trough plants, *Sol. Energy* (2001).
- [26] Concentrating solar power projects | NREL. <https://solarpaces.nrel.gov/>. (Accessed 4 March 2023).
- [27] B. Haddad, P. Diaz-Cuevas, P. Ferreira, A. Djebli, J.P. Pérez, Mapping concentrated solar power site suitability in Algeria, *Renew. Energy* 168 (May 2021) 838–853, <https://doi.org/10.1016/j.renene.2020.12.081>.
- [28] L. Sun, et al., A GIS-based multi-criteria decision making method for the potential assessment and suitable sites selection of PV and CSP plants, *Resour. Conserv. Recycl.* 168 (May 2021), 105306, <https://doi.org/10.1016/j.resconrec.2020.105306>.
- [29] G. Ghasemi, Y. Noorollahi, H. Alavi, M. Marzband, M. Shahbazi, Theoretical and technical potential evaluation of solar power generation in Iran, *Renew. Energy* 138 (Aug. 2019) 1250–1261, <https://doi.org/10.1016/j.renene.2019.02.068>.
- [30] M.B. Alqaderi, W. Emar, Oa, Concentrated solar power site suitability using GIS-MCDM technique taken UAE as a case study, *Int. J. Adv. Comput. Sci. Appl.* 9 (4) (2018), <https://doi.org/10.14569/IJACSA.2018.090440>.
- [31] A. Alami Merrouni, F. Elwali Elaloui, A. Ghennioui, A. Mezrhah, A. Mezrhah, A GIS-AHP combination for the sites assessment of large-scale CSP plants with dry and wet cooling systems. Case study: eastern Morocco, *Sol. Energy* 166 (May 2018) 2–12, <https://doi.org/10.1016/j.solener.2018.03.038>.
- [32] G. Tazi, O. Bjaïhi, A. Ghennioui, A.A. Merrouni, M. Bakkali, Estimating the Renewable Energy Potential in Morocco: solar energy as a case study, *IOP Conf. Ser. Earth Environ. Sci.* 161 (1) (Jun. 2018), 012015, <https://doi.org/10.1088/1755-1315/161/1/012015>.
- [33] A. Aly, S.S. Jensen, A.B. Pedersen, Solar power potential of Tanzania: identifying CSP and PV hot spots through a GIS multicriteria decision making analysis, *Renew. Energy* 113 (Dec. 2017) 159–175, <https://doi.org/10.1016/j.renene.2017.05.077>.
- [34] M. Giamalaki, T. Tsoutsos, Sustainable siting of solar power installations in Mediterranean using a GIS/AHP approach, *Renew. Energy* 141 (Oct. 2019) 64–75, <https://doi.org/10.1016/j.renene.2019.03.100>.
- [35] T.L. Saaty, L.G. Vargas, Estimating technological coefficients by the analytic hierarchy process, *Socioecon. Plann. Sci.* 13 (6) (Jan. 1979) 333–336, [https://doi.org/10.1016/0038-0121\(79\)90015-6](https://doi.org/10.1016/0038-0121(79)90015-6).
- [36] B. Mutume, D. Alp, Coal bed methane gas in-place estimation for the North-Western region of Zimbabwe, *Nat. Gas. Ind. B* 10 (1) (Feb. 2023) 86–101, <https://doi.org/10.1016/j.ngib.2023.01.001>.
- [37] SOLARGIS, 'Solar Irradiance data'. <https://solargis.com/> (accessed December. 4, 2022).
- [38] Data | U.S. Geological survey. <https://www.usgs.gov/products/data>. (Accessed 4 December 2022).
- [39] World Bank open data | data. <https://data.worldbank.org/>. (Accessed 4 December 2022).
- [40] Download free Zimbabwe country, city, region, boundaries GIS shapefile map layers. <https://mapcruzin.com/free-zimbabwe-country-city-place-gis-shapefiles.htm>. (Accessed 4 December 2022).
- [41] British Geological Survey, Africa groundwater. <https://www2.bgs.ac.uk/africagroundwateratlas/index.html>. (Accessed 2 December 2022).
- [42] Z. Wang, Chapter 7 - site selection, power load, and power generation procedures, in: Z. Wang (Ed.), *Design of Solar Thermal Power Plants*, Academic Press, 2019, pp. 417–424, <https://doi.org/10.1016/B978-0-12-815613-1.00007-9>.
- [43] L. Qoaider, A. Liqueina, Optimization of dry cooled parabolic trough (CSP) plants for the desert regions of the Middle East and North Africa (MENA), *Sol. Energy* 122 (Dec. 2015) 976–985, <https://doi.org/10.1016/j.solener.2015.10.021>.
- [44] Home - system advisor model - SAM. <https://sam.nrel.gov/>. (Accessed 19 May 2023).
- [45] Microsoft Excel spreadsheet software | microsoft 365. <https://www.microsoft.com/en/microsoft-365/excel>. (Accessed 11 March 2023).
- [46] S. Henbest, L. Mills, I. Orlandi, A. Serhal, R. Pathania, Levelised cost of electricity: DFID 28 priority countries, Accessed: Dec. 23, 2022. [Online]. Available: <https://www.gov.uk/research-for-development-outputs/levelised-cost-of-electricity-dfid-28-priority-countries>.
- [47] ZESA Increases Electricity Tariffs Effective 15 May 2022, *Energy Central*, May 16, 2022. <https://energycentral.com/news/zesa-increases-electricity-tariffs-effective-15-may-2022>. (Accessed 4 December 2022).
- [48] G. Dzoma, ZESA Increases Tariffs Starting 6 October 2022, *Zimpricecheck*, Oct. 08, 2022. <https://zimpricecheck.com/market-intelligence/zesa-increases-tariffs-starting-6-october-2022/>. (Accessed 4 December 2022).